The final publication is available at

http://doi.org/10.1061/(ASCE)WW.1943-5460.0000322

Additional Information

Explicit Wave-Overtopping Formula for Mound Breakwaters with Crown Walls Using CLASH Neural Network–Derived Data

Jorge Molines [a],* and Josep R. Medina [b]

[a] Research Assistant, Dept. of Transportation, ETSI Caminos, *Universitat Politècnica de València*, Camino de Vera s/n, 46022 Valencia, Spain. E-Mail: jormollo@upv.es (*corresponding author)

[b] Professor, Dept. of Transportation, ETSI Caminos, *Universitat Politècnica de València*, Camino de Vera s/n, 46022 Valencia, Spain. E-Mail: jrmedina@upv.es

ABSTRACT

Based on the CLASH Neural Network (CLASH NN), a new 16-parameter overtopping estimator (*Q6*) is developed for conventional mound breakwaters with crown wall, both with and without toe berm. *Q6* is built-up using the overtopping estimations given by the CLASH NN and checked using the CLASH database. *Q6* is compared to other conventional overtopping formulas, and the *Q6* obtained the lowest predicting errors. *Q6* provides overtopping predictions similar to the CLASH NN for CMBW but using only six explanatory dimensionless variables *(R_c/H_{m0}, Ir, R_c/h, G_c/H_{m0}, A_c/R_c and a toe berm variable based on R_c/h)* and two reduction factors (γ_f and γ_β). *Q6* describes explicit relationships between input variables and overtopping discharge and hence it facilitates use in engineering design to identify cost-effective solutions and to quantify the influence of variations in wave and structural parameters.

Keywords: Wave overtopping; Mound breakwater; Neural network; CLASH database; Crown wall; EurOtop

Introduction

The European CLASH Project (2001-2003) collected data from 10,532 overtopping tests, conducted in a number of laboratories (see Verhaeghe et al., 2003 and Van der Meer et al., 2009) and corresponding to a variety of coastal structures. An overtopping predicting model based on artificial neural networks, described by Van Gent et al. (2007), was developed using most of the CLASH database. The CLASH NN is able to predict the mean overtopping discharge and the associated confidence intervals for almost any type of coastal structure. The CLASH NN is routinely used by consultants in the preliminary stage of breakwater design and by scientists in small-scale experiments. Fig. 1 illustrates the 15 structural and environmental input parameters which define a general case for the CLASH NN. Variables given in Fig. 1 and Fig. 2 are defined as follows: R_c is the crown wall freeboard; A_c is the armor crest freeboard; G_c is the armor crest berm width; $\cot\alpha_d$ is the slope of the structure downward from the berm; $\cot\alpha_u$ is the slope of the structure upward from the berm; B is the width of the berm; $\cot\alpha_b$ is the slope of the berm; h_b is the water depth on the berm; h is the water depth in front of the structure; h_t is the water depth at the toe of the structure; B_t is the width of the toe berm; β is the angle of wave attack; $H_{m0}=4(m_0)^{1/2}$ is the significant wave height at the toe of the structure; $T_{-1,0}=m_{-1}/m_0$ is the mean spectral wave period at the toe of the structure, being m_n the nth spectral moment, and γ_f is the roughness factor of the armor layer.
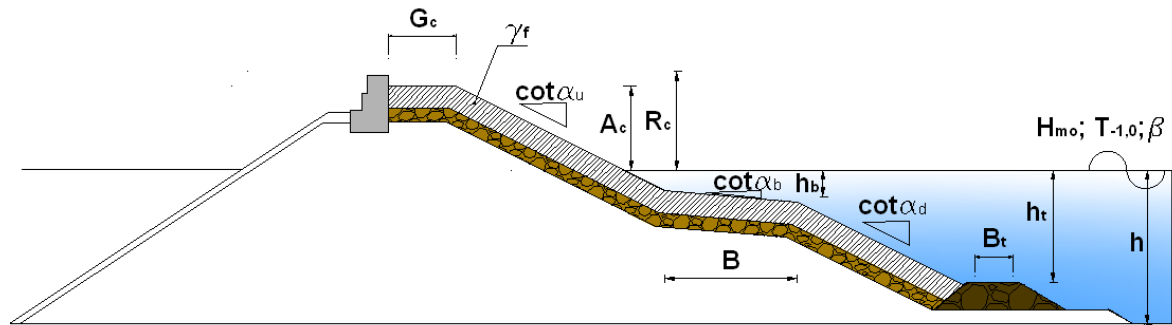
Figure 1. CLASH breakwater cross-section considered for the CLASH NN predictor.

This research focuses on conventional mound breakwaters (CMBW) with crown walls and with and without toe berms, corresponding to the cross-section depicted in Fig. 2. This is the most common typology for mound breakwaters, especially when concrete armor units are used.

Molines and Medina (2015) compared different overtopping estimators and found that the CLASH NN performed better in comparison to other estimators; however, it is a "black-box" which does not clarify how overtopping is affected by specific explanatory variables. This paper describes a methodology to build-up a new and explicit overtopping formula which can provide predictions for CMBW in non-breaking conditions. The new formula Q6 estimates overtopping almost as well as the CLASH NN, but without being a "black-box". Q6 provides explicit descriptions of the relationships between input variables and the overtopping rate on CMBW and allows for a better understanding of how specific structural and wave characteristics influence wave overtopping. The formula was obtained from systematic simulations using the CLASH NN, and it was validated with the test results of the CLASH database corresponding to the CMBW typology.
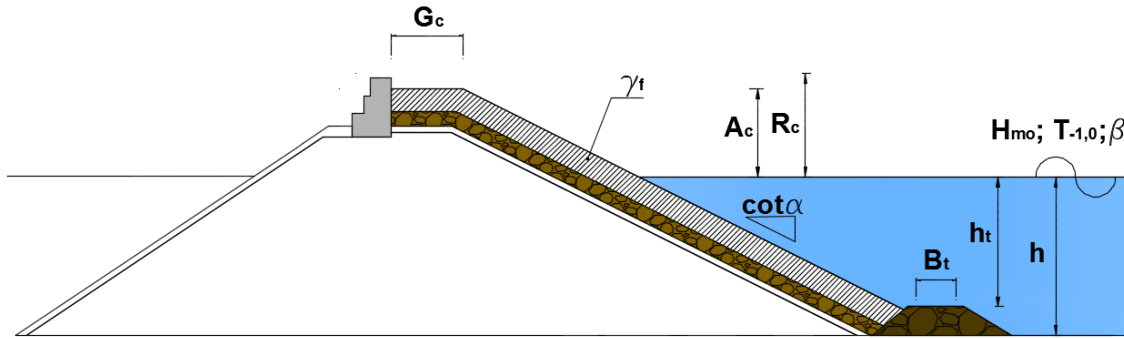
Figure 2. Conventional mound breakwater cross-section with crown wall.

This paper is structured as follows. A technical overtopping background is given first. Secondly, the structural and environmental variables affecting overtopping on CMBW are described as are the tests extracted from the CLASH database. Thirdly, the methodology to build-up the formula corresponding to the CLASH NN is explained in detail. Fourthly, the confidence intervals of the new formula are calculated. Fifthly, a sensitivity analysis is conducted and the influence of the breakwater geometry on overtopping is highlighted. Sixthly, different overtopping formulas given in the literature are compared with the new Q6 and the neural network overtopping estimator. Finally, general conclusions are drawn.

Overtopping formulas

USACE (2002) listed numerous overtopping formulas, dimensionless overtopping discharge and dimensionless input variables described in the literature, including those by Owen (1980), Aminti and Franco (1988), Bradbury and Allsop (1988), Van der Meer and Janssen (1994) and Pedersen (1996).

In the general exponential model given by Eq. (1), the dimensionless overtopping variable $Q=q/[gH_{m0}^3]^{1/2}$ and the dimensionless input variable $R=R_c/H_{m0}$ appear to be the dimensionless variables most often used in recent studies on wave overtopping.

$$Q = A_1 \cdot \exp(-A_2 \cdot R)$$ (1)

where A_1 and A_2 are empirical coefficients provided in the literature; Q is the dimensionless mean overtopping discharge, R is the dimensionless crest freeboard, q is the mean overtopping discharge per meter structure width and g is the gravity acceleration.

Eq. (2) was proposed by Van der Meer and Janssen (1994) to estimate wave overtopping on dikes in non-breaking conditions. Eq. (2) is an Eq. (1)-type exponential model with $Q=q/[gH_{m0}^3]^{1/2}$ and $R= R_c/(\gamma_f \gamma_\beta H_{m0})$.

$$Q_{VMJ} = \frac{q}{\sqrt{g \cdot H_{m0}^3}} = B_1 \cdot \exp\left(-B_2 \cdot \frac{R_c}{H_{m0}} \cdot \frac{1}{\gamma_f \gamma_\beta}\right)$$ (2)

where $B_1 = 0.2$; $B_2 = 2.6$; γ_f and γ_β are reduction factors to account for the effect of the slope roughness and the oblique wave attack, respectively. Eq. (2) is a simple and robust formula with only two parameters. The corresponding ranges of application for the slope angle, relative crown wall freeboard and Iribarren's number in Eq. (2) are as follows: $1.0 < \cot\alpha < 4.0$; $0.5 < R_c/H_{m0} < 3.5$ and $Ir_p= \tan\alpha/[2\pi H_{m0}/gT_p^2]^{1/2} > 2$. The reliability of Eq. (2) is expressed by considering $B_2 = 2.6$ as a normally distributed random variable $N(2.6, 0.35^2)$.

EurOtop (2007) suggested using Eq. (2) to calculate an initial approximation to overtopping discharge and then correct this first estimation with Eqs. (3a) and (3b) proposed by Besley (1999) if $G_c>3D_{n50}$ (where D_{n50} is the armor unit equivalent cube size length or nominal diameter).

$$Cr = \min\left[1.0; C_1 \cdot \exp\left(-C_2 \cdot \frac{G_c}{H_{m0}}\right)\right] \qquad (3a)$$

$$Q_{EurOtop} = \frac{q}{\sqrt{g \cdot H_{m0}^3}} = Cr \cdot Q_{VMJ} \qquad (3b)$$

where Cr is the reduction factor; C_1 = 3.06, and C_2 = 1.5. Eq. (3a) was derived by Besley (1999) to correct the estimations given by Owen (1980) for rock slopes and $R_c = A_c$. Besley (1999) reported that Eq. (3a) can be conservatively applied to other permeable structures.

For cube- and Cubipod®-armored CMBW, Smolka et al. (2009) proposed the following overtopping formula:

$$Q_{SZM} = \frac{q}{\sqrt{g \cdot H_{m0}^3}} = D_1 \cdot \exp\left(D_2 \cdot Ir_p - D_3 \cdot \frac{A_c}{R_c} - D_4 \frac{R_c}{H_{m0}} \cdot \frac{1}{\gamma_f}\right) \qquad (4)$$

where D_1=0.2; D_2=0.53; D_3=3.27; D_4=2.16; Ir_p=$\tan\alpha/[2\pi H_{m0}/gT_p^2]^{1/2}$ with T_p the peak period considering γ_f [cube, 2 Layers randomly-placed] =0.50; γ_f [Cubipod®, 1 Layer] =0.46 and γ_f [Cubipod®, 2 Layers] =0.44. The ranges of application are as follows: 2.7< Ir_p <7.0, cotα=1.5, 0.70<A_c/R_c [cube, 2 Layers randomly-placed]<1.00, 0.40<A_c/R_c [Cubipod®, 1 Layer]<0.65, 0.58<A_c/R_c [Cubipod®, 2 Layers]<0.80, and 1.30<R_c/H_{m0}<2.80.

Molines et al. (2012) studied wave overtopping on sections under construction when the crown wall freeboard takes on relatively low values. Two formulas similar to Eq. (4) were proposed to estimate wave overtopping on cube- and Cubipod®-armored breakwaters. The variable R_c/h was statistically significant in both formulas. Armor damage was also a relevant variable for cube-armored breakwaters.

Victor and Troch (2012) studied wave overtopping on smooth impermeable steep slopes with low crest freeboards, and attempted to increase the efficiency of wave energy generation. They proposed prediction formulas similar to Eq. (2) to consider the effects of slope angle and a small relative crest freeboard in non-breaking conditions.

Jafari and Etemad-Shahidi (2012) and Etemad-Shahidi and Jafari (2014) used the CLASH database and model tree techniques to develop prediction formulas for wave overtopping on rubble mound structures and smooth slopes, respectively. Model trees divide the initial complex problem into small subdomains where multiple linear regression techniques similar to Eq. (4) were applied. These authors proposed Eq. (5) for rough slopes.

$$
\begin{cases}
if \ \dfrac{R_c}{H_{m0}} > E_1 \ and \ \dfrac{G_c}{H_{m0}} > E_2 \ then \ Q_{JE} = \dfrac{q}{\sqrt{g \cdot H_{m0}^3}} = \exp\left(-E_3 \dfrac{R_c}{\gamma_f \gamma_\beta H_{m0}} \dfrac{\sqrt{s_{0p}}}{\tan \alpha} - E_4 \tan \alpha - E_5 \right) \\[3mm]
if \ \dfrac{R_c}{\gamma_f \gamma_\beta H_{m0}} \dfrac{\sqrt{s_{0p}}}{\tan \alpha} \le E_6 \ then \ Q_{JE} = \dfrac{q}{\sqrt{g \cdot H_{m0}^3}} = \exp\left(-E_7 \dfrac{R_c}{\gamma_f \gamma_\beta H_{m0}} \dfrac{\sqrt{s_{0p}}}{\tan \alpha} - E_8 \right) \\[3mm]
if \ \dfrac{R_c}{\gamma_f \gamma_\beta H_{m0}} \dfrac{\sqrt{s_{0p}}}{\tan \alpha} > E_6 \ then \ Q_{JE} = \dfrac{q}{\sqrt{g \cdot H_{m0}^3}} = \exp\left(-E_9 \dfrac{R_c}{\gamma_f \gamma_\beta H_{m0}} \dfrac{\sqrt{s_{0p}}}{\tan \alpha} - E_{10} \tan \alpha - E_{11} \right)
\end{cases}
\tag{5}
$$

where E_1=2.08; E_2=1.51; E_3=0.6396; E_4=0.7085; E_5=11.4897; E_6=0.86; E_7=6.18; E_8=3.21; E_9=3.1; E_{10}=6.05; E_{11}=2.63 and s_{0p}=H_{m0}/L_{0p} is the wave steepness using L_{0p}=$gT_p^2/(2\pi)$. The ranges of application of Eq. (5) are given in Table 1.

Van der Meer and Bruce (2014) proposed modifying the Q_{VMJ} formula to estimate overtopping on sloping structures in non-breaking conditions, valid in a wider range of application, $R_c \ge 0$:

$$
Q_{VMB} = \dfrac{q}{\sqrt{g \cdot H_{m0}^3}} = F_1 \cdot \exp\left(-\left(F_2 \cdot \dfrac{R_c}{H_{m0}} \cdot \dfrac{1}{\gamma_f \gamma_\beta} \right)^{F3} \right)
\tag{6}
$$

where F_1=0.09, F_2=1.5, and F_3=1.3. Van der Meer and Bruce (2014) noted that Eq. (6) provides overtopping discharge estimations similar to Eq. (2), but better estimations for low and zero

crown wall freeboards (R_c/H_{m0}<0.5). The reliability of Eq. (6) is expressed by considering $F_1 =$ 0.09, as a normally distributed random variable N(0.09, 0.013²) and $F_2 =$ 1.5 as N(1.5, 0.15²).

Van Doorslaer et al. (2015) analyzed the influence of crest modifications to reduce wave overtopping of non-breaking waves over a smooth dike slope, deriving several correction factors to be applied to an Eq.(2)-type overtopping estimator.

Molines and Medina (2015) analyzed different overtopping estimators for CMBW and found that the CLASH NN estimator had a far superior performance compared to Eqs. (2) to (4) and Eq. (6); a methodology was given to estimate the γ_f for a specific formula and database, providing the optimum γ_f to be considered when using different overtopping estimators. Simple empirical formulas with few parameters require the roughness factor (γ_f) to account for structural and wave information which is not explicitly included in the formula.

Order (j)	Variable (X_j)	Min.-Max.					
		Eq. (2)	Eqs. (3)	Eq. (4)	Eq. (5)	Eq. (6)	Q6
1	R_c/H_{m0}	0.50 - 3.50	0.50 - 3.50	1.30 - 2.80	0.50 – 2.59	0.00 - 3.50	0.52 - 3.75
2	Ir	$Ir_p \geq 2$	$Ir_p \geq 2$	2.70≤Ir_p≤7.00	1.31≤Ir_p≤9.27	$Ir_p \geq 2$	1.65 - 7.21
3	R_c/h	-	-	-	-	-	0.09 - 1.34
4	G_c/H_{m0}	-	0.00 - 6.50	-	0.00 - 3.88	-	0.00 - 3.50
5	A_c/R_c	-	-	0.40 - 1.00 (depending on armor unit)	-	-	0.38 - 1.38
6	B_t/H_{m0}	-	-	-	-	-	0.00 - 15.9
7	h_t/H_{m0}	-	-	-	-	-	1.45 - 17.5

Table 1. Range of application of Eqs.(2) to Eq.(6) and Q6.

Explanatory variables affecting overtopping on CMBW

In this paper, we considered the 11 input variables of the CLASH NN for CMBW (Fig. 2) and selected 7 dimensionless variables as candidates which may significantly influence overtopping discharge on CMBW:

1. R_c/H_{m0} (dimensionless crown wall freeboard) is the most common and widely accepted dimensionless variable which mainly controls the overtopping discharge. The effects of roughness slope and oblique waves are usually considered using the roughness factor ($\gamma_f \leq 1.0$) and obliquity factor ($\gamma_\beta \leq 1.0$), respectively; γ_f and γ_β, are used as reduction factors in the significant wave height as $R_c/(\gamma_f\ \gamma_\beta\ H_{m0})$. The higher the γ_f or γ_β, the higher the overtopping rates. The CLASH EU-Project identified different white spots such as the effect of wave obliqueness, short-crested waves and directional spreading (s) on overtopping. Lykke-Andersen and Burcharth (2004 and 2009) conducted specific tests on cube and rock armored mound breakwaters within the CLASH EU-Project to derive the γ_β for short-crested ($s>0$) and long-crested waves ($1/s=0$).

2. $Ir= \tan\alpha/[2\pi H_{m0}/gT^2_{-1,0}]^{1/2}$ (Iribarren's number or breaker parameter using H_{m0} and $T_{-1,0}$ at the toe of the structure) is a variable widely used in coastal engineering. Ir takes into account the influence of wave steepness and structure slope angle, determining the type of wave breaking on the slope. The influence of wave steepness, slope angle or Ir on overtopping were reported by Pedersen (1996), Hebsgaard et al. (1998) and Medina et al. (2002), among others. Bruce et al. (2009) concluded that γ_f increases with Ir and thus Ir affected the overtopping rates. In the present study, wave steepness and slope angle were analyzed separately to determine if Ir reasonably integrates the influence of both variables on the overtopping discharge.

3. R_c/h (relative water depth) is a variable which relates the crown wall freeboard with the

water depth. It was used by Molines et al. (2012) to study wave overtopping on CMBW during

construction. This variable includes the information about the water depth, which can be

valuable for overtopping estimations of CMBW with deep armors, such as those existing during

the construction phase.

4. G_c/H_{m0} (relative armor crest berm width) is a variable which considers the armor crest

berm width of the breakwater. It was used by Besley (1999) and recommended by EurOtop

(2007) in the reduction factor Cr given by Eq. (3a). Wide crest berms lead to high energy

dissipation and hence a low overtopping discharge.

5. A_c/R_c (relative armor crest freeboard) is a variable to relate the armor crest freeboard with

the crown wall freeboard [used by Smolka et al. (2009)]. High values for A_c mean high crests

which lead to high energy dissipation and thus a low overtopping rate.

6. B_t/H_{m0} (relative toe berm width) is a variable describing the toe berm width, which may

influence overtopping discharge.

7. h_t/H_{m0} (relative toe depth) is a variable used in the CMBW design rules given by Grau

(2008). This dimensionless variable is related to the depth of the toe berm, which may influence

overtopping discharge.

Overtopping tests considered in the present study

Two sets of data corresponding to CMBW were considered from the CLASH database

(http://www.clash.ugent.be/ [Accessed: December 2014]), having β=0º (1,307 data) and

β>0º(561 data)

For perpendicular wave attack (β=0º), the data filter applied was the same as that detailed by Molines and Medina (2015): β=0º; cotα_d=cotα_u=cotα; 1.19 ≤cotα ≤ 4; B=0; tanα_b=0; h_b=0; CF (Complexity Factor)=1; RF (Reliability Factor)≤2; non-breaking conditions and Q>10^{-6}. Additionally, the Cubipod® tests conducted by Smolka et al. (2009) were analyzed in the present study. 1,307 tests corresponding to CMBW were considered. In the present study, CLdata refers to the 1,307 measured overtopping discharges of tests with β=0º and NNdata to the 1,307 predicted overtopping discharges by the CLASH NN of tests with β=0º. The ranges of the variables for CMBW derived from the selected tests are specified in Table 1, together with the applicability range of the formula given herein.

For oblique wave attack (10º≤β≤60º), 561 tests reported by Lykke-Andersen and Burcharth (2004 and 2009) were used in this paper since: (1) they were specifically conducted within the CLASH EU-Project to analyze the effect of oblique waves on overtopping and (2) they constitute 90% of the tests with β>0º corresponding to CMBW in the CLASH database. Tests with β>0º were not used when building-up the estimator Q6, which was calibrated only with tests with β=0º. Tests with oblique wave attack were only used for the final estimator Q6.

The relative Mean Squared Error (*rMSE*) of log Q is a dimensionless *MSE*, similar to that used in Van Gent et al. (2007) for the CLASH NN estimator, and is used in this study to measure the goodness of fit:

$$rMSE_e\left(\log Qo\right) = \frac{MSE_e\left(\log Qo\right)}{Var(\log Qo)} = \frac{\sum_{i=1}^{N} WF_i\left(\log Qe_i - \log Qo_i\right)^2}{\left(\sum_{i=1}^{N} WF_i\right) \cdot Var\left(\log Qo\right)} \qquad (7)$$

where "*e*" refers to the overtopping estimator; *Qe* and *Qo* are the estimated and target dimensionless mean overtopping rate, respectively; *N* is the total number of data; *i* is the data index (i=1,2,….,N); *WF* is the weight factor depending on the Reliability Factor given in Table 2 as specified in the CLASH EU-Project (see Van Gent et al., 2007).

RF	*WF*
1	9
2	6

Table 2. Weight Factor dependent on the Reliability Factor.

The *rMSE* falls in the range 0%<*rMSE_e*(log *Qo*)<100%, indicating the proportion of variance of the data (log *Qo*) which is not explained by the estimator "e".

Fig. 3 illustrates the performance of the CLASH NN estimator with the roughness factor given by Molines and Medina (2015) for the ranges of applications given by Table 1. The low rMSE=8.1% indicates that the CLASH NN estimator accurately predicts the overtopping rates on CMBW with β=0° given in CLASH database; these predictions are abbreviated as NNdata.

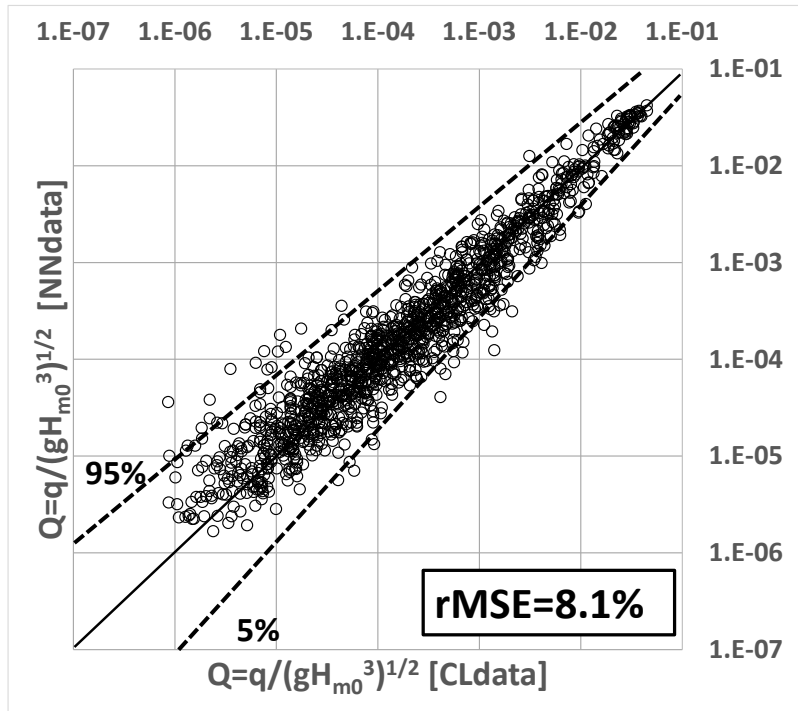*Figure 3. Measured overtopping rate with β=0 $_o$ (CLdata) compared to predicted overtopping rate using the CLASH NN.*

Methodology

General outline

The methodology described herein was used to obtain an explicit formula from the CLASH NN model, and it is similar to the methodology used by both Medina et al. (2002) to predict overtopping, and Garrido and Medina (2012) to estimate the coefficient of reflection of Jarlan-type breakwaters. The methodology does not guarantee the exact same result when using the same database and explanatory variable list, but it does provide an explicit formula which may successfully emulate the neural network "black-box" estimator.

The new neural network-derived explicit formula was built-up by consecutively introducing each dimensionless variable X_j (j=1, 2, etc.) given in Table 1. The overtopping estimator after

introducing each variable was referred to as $Qj = Q(X_1, X_2,….., X_j)$. The process of building-up the formula started with Eq. (2) as the first overtopping predictor $Q1 = Q(X_1)$, which only considers the influence of the variable $X_1 = R_c/H_{m0}$. Q1 has only two parameters in Eq. (8) equivalent to Eq. (2).

Secondly, overtopping simulations were carried out with the CLASH NN varying $X_2 = Ir$ and using constant values of X_1 and X_3 to X_7. The qualitative analysis of a graphic representation of the neural network overtopping simulations (Q_{CLNN}) allowed for the recommendation of an estimator $Q2 = Q(X_1, X_2)$. Parameters were calibrated to minimize (1) rMSE$_{Q2}$ (CLdata), (2) rMSE$_{Q2}$ (NNdata) and (3) the number of significant figures. Variables X_3, X_4, and so on were considered similarly to build-up estimators $Q3$, $Q4$, and so on. Simulations were conducted using the following indicative constant values of the variables: R_c/H_{m0}=0.80,1.00,1.20,1.50,2.00 (five values); Ir=3.50; R_c/h=0.25; G_c/H_{m0}=1.00; A_c/R_c=1.00; B_t/H_{m0}=0.00 and $h/H_{m0}=h_t/H_{m0}$ (no toe berm); $\gamma_f = 0.47$ and, $\beta=0°$. The simulations of the CLASH NN served as basis to build-up the new overtopping predictor Q6, which was validated using all the CMBW cases selected from the CLASH database. Fig. 4 gives a flow-chart to summarize the methodology used for this study.
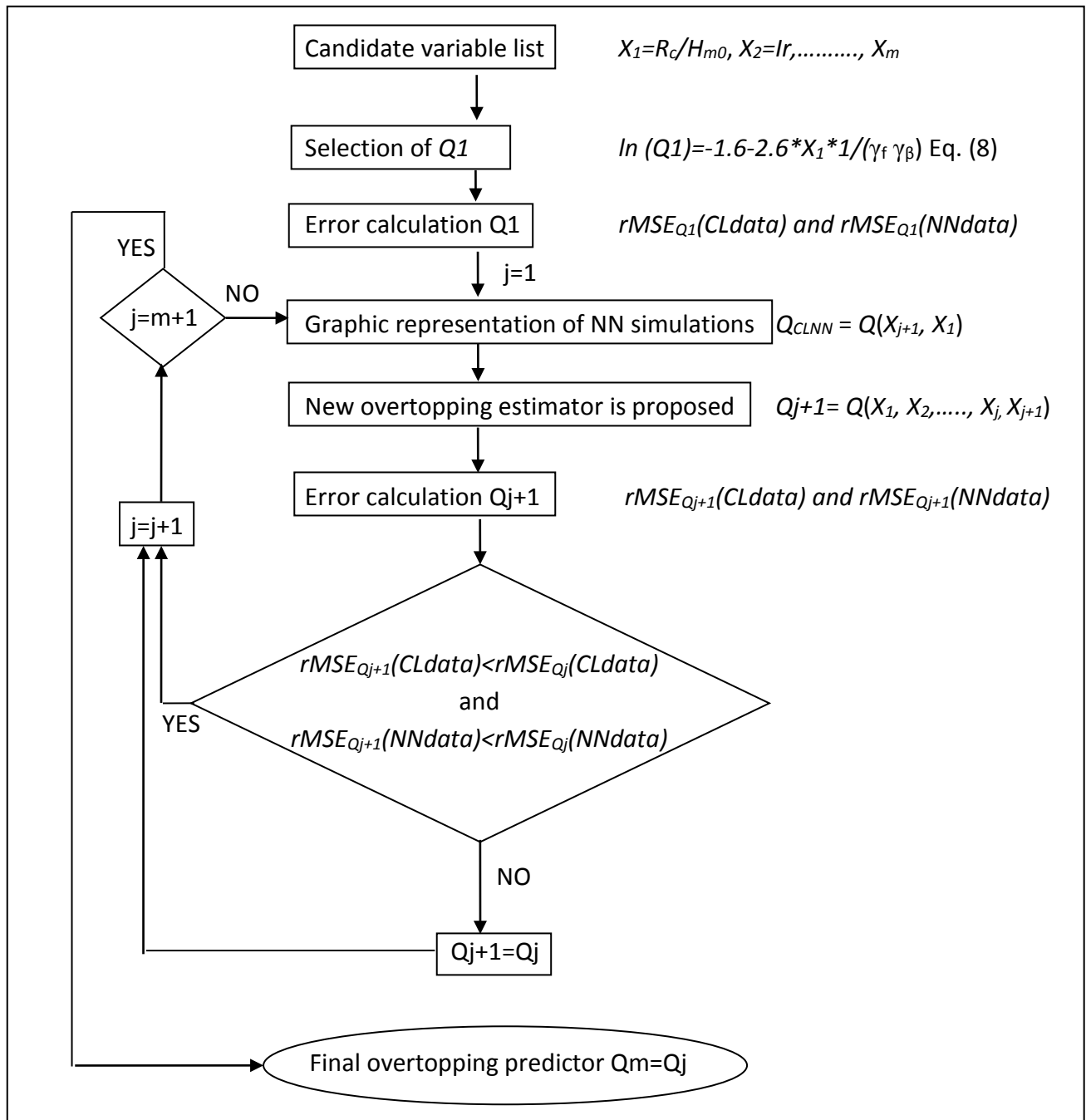
Figure 4. Flow-chart to build-up the new overtopping estimator Q6.

Dimensionless crown wall freeboard, $X_1 = R_c/H_{m0}$. Initial formula

It is widely accepted in the literature that $X_1 = R_c/H_{m0}$ is the main variable governing overtopping phenomenon. Eq. (2) may be rewritten as follows:

$$\ln Q1 = \ln\left(\frac{q}{\sqrt{g \cdot H_{m0}^3}}\right) = a_1 + b_1 \frac{R_c}{H_{m0}} \cdot \frac{1}{\gamma_f \gamma_\beta} \tag{8}$$

where $a_1 = -1.6$ and $b_1 = -2.6$. The roughness factor was taken initially as the best fitted value for the CLASH NN model given by Molines and Medina (2015), so for the final estimator Q6, the γ_f was then derived specifically following their methodology.

Lykke-Andersen and Burcharth (2009) reported that the CLASH NN predicted overtopping of short-crested waves very well in the entire range of obliqueness, but overpredicted overtopping of long-crested waves for $\beta > 45°$ (outside the range of validity of the CLASH NN). The obliquity factor given by Lykke-Andersen and Burcharth (2009) for short-crested and long-crested waves was applied in this study for the final estimator Q6 on the 561 tests selected from the CLASH database with $10° \leq \beta \leq 60°$.

In the present study, Eq. (8) was considered the initial formula to predict mean overtopping discharge on CMBW; $rMSE_{Q1}$ (CLdata) = 41.2% and $rMSE_{Q1}$ (NNdata) = 42.2%. Fig. 5 compares the overtopping rate in CLdata with estimations $Q1 = Q(X_1)$, given by Eq. (8); the general trend is well defined by Eq. (8). Thus, Eq. (8), equivalent to Eq. (2), was taken as the initial formula to be modified adding new explanatory variables.
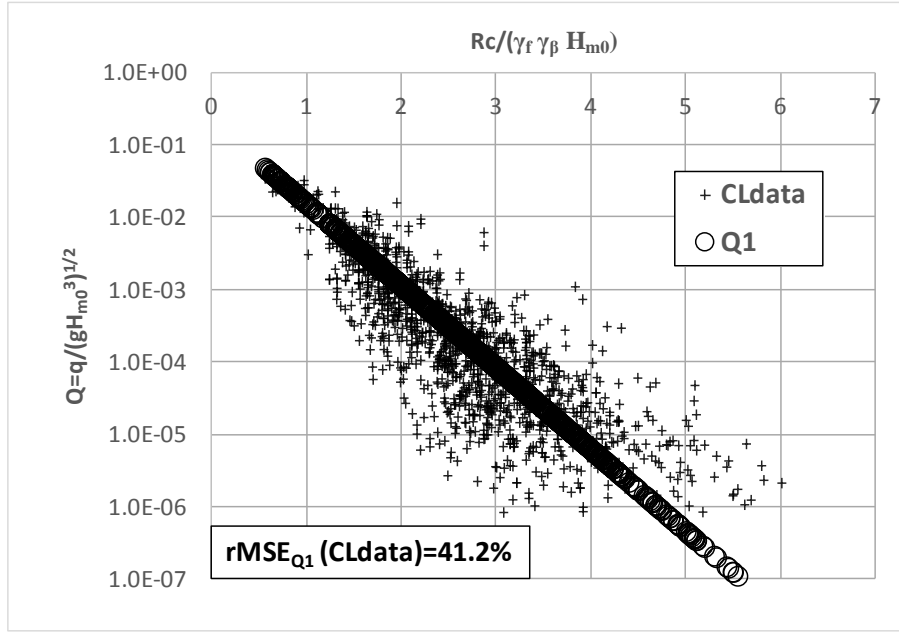
Figure 5. Overtopping rate in CLdata compared to that predicted by Q1.

Each new variable X_j (j=2 to 7) was added as a new explanatory term for Eq. (8). The general structure of the overtopping formula is expressed in (9):

$$\ln Q j = (\lambda_2 \cdot \lambda_3 ...... \lambda_j) \cdot [\ln Q1] \qquad (9)$$

where λ_j is the j-th explanatory term corresponding to the variable X_j (j=2 to 7). The predicted overtopping discharge increases if $\lambda_j<1$ (ln($Q1$)<0).

Iribarren's number, $X_2=Ir$

The Iribarren number or breaker parameter, $Ir=\tan\alpha/[2\pi H_{m0}/gT^2_{-1,0}]^{1/2}$, depends on two independent dimensionless variables: (1) armor slope angle (α) and (2) deep water wave steepness ($H_{m0}/L_{0,-1}= [2\pi H_{m0}/gT^2_{-1,0}]$) with H_{m0} and $T_{-1,0}$ measured at the breakwater toe. To determine the influence of each variable, two sets of simulations were considered: one varying the armor slope (Fig. 6a) and the other varying wave steepness (Fig. 6b).
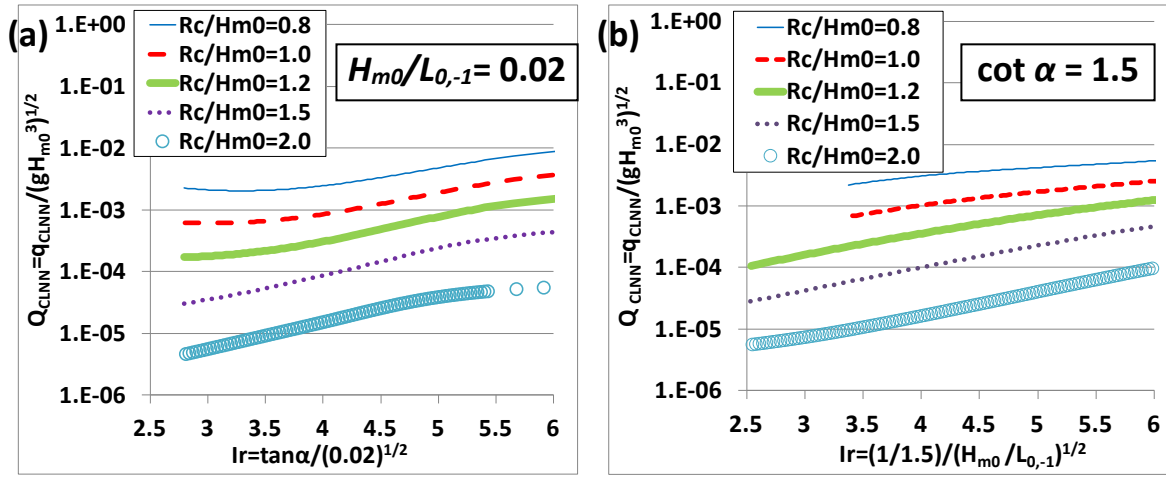
Figure 6. Influence of Ir on log Q if (a) wave steepness or (b) slope angle are constant.

Fig. 6 shows that both armor slope (cotα) and wave steepness ($H_{m0}/L_{0,-1}$) significantly influence the overtopping rate. Thus, Iribarren's number (Ir) seems to be a reasonable variable to account for the influence of armor slope and wave steepness simultaneously.

The interaction between $X_1=R_c/H_{m0}$ and $X_2=Ir$ was analyzed to improve the explanatory term using only two parameters. The explanatory term using the variable $Ir[R_c/H_{m0}]^{1/2}$ (Fig. 7b) was found to be a better descriptor than that obtained using only Ir (Fig. 7a).
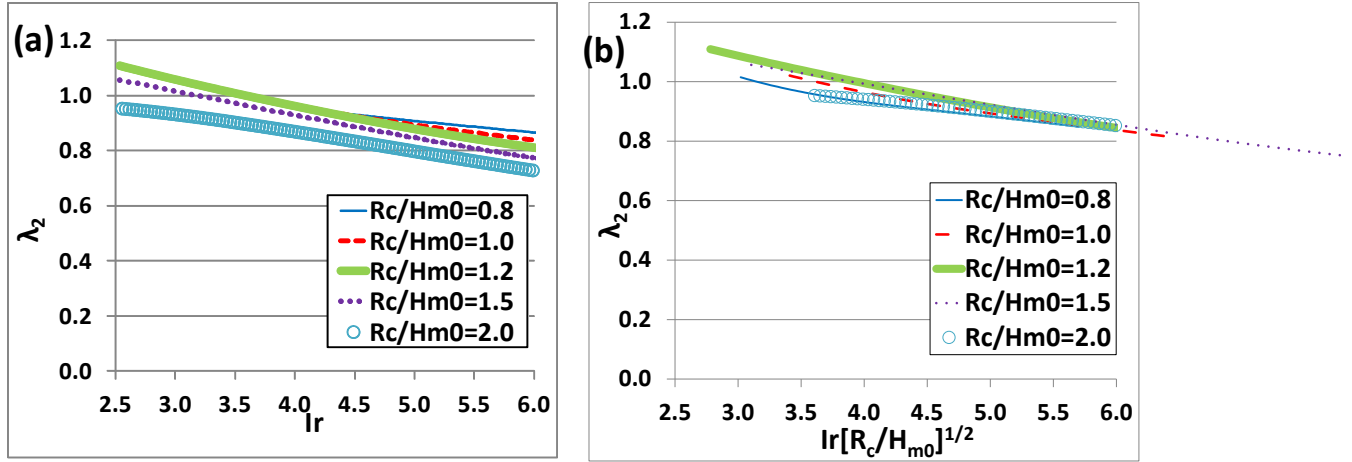
Figure 7. Explanatory term λ2 as function of (a) Ir or (b) Ir[Rc/Hm0]¹/².

The overtopping prediction of Q2 is given by:

$$\ln Q2 = \lambda_2 \ln Q1 = [a_2 + b_2 \cdot \left(Ir\sqrt{R_c/H_{m0}} \right)] \cdot \ln Q1 \qquad (10)$$

where a_2 = 1.20 and b_2 = -0.05; rMSE$_{Q2}$ (CLdata) = 26.1% << 41.2% = rMSE$_{Q1}$ (CLdata) and

rMSE$_{Q2}$ (NNdata) = 21.8% << 42.2% = rMSE$_{Q1}$ (NNdata). Eq. (10) clearly improves the

overtopping prediction given by Eq. (8). The Iribarren number (Ir=tanα/[2πH_{m0}/g$T^2_{-1,0}$]$^{1/2}$) is a

relevant variable to explain the mean overtopping discharge on CMBW; the higher the Ir, the

higher the overtopping discharge. The predicted overtopping discharge increases if λ_2<1

($\ln(Q1)$<0).

Dimensionless water depth, X_3=R_c/h

Fig. 8a is a graphic representation of overtopping simulations using the CLASH NN. The lower

the X_3=R_c/h, the greater the impact on overtopping. The explanatory term λ_3 is represented in
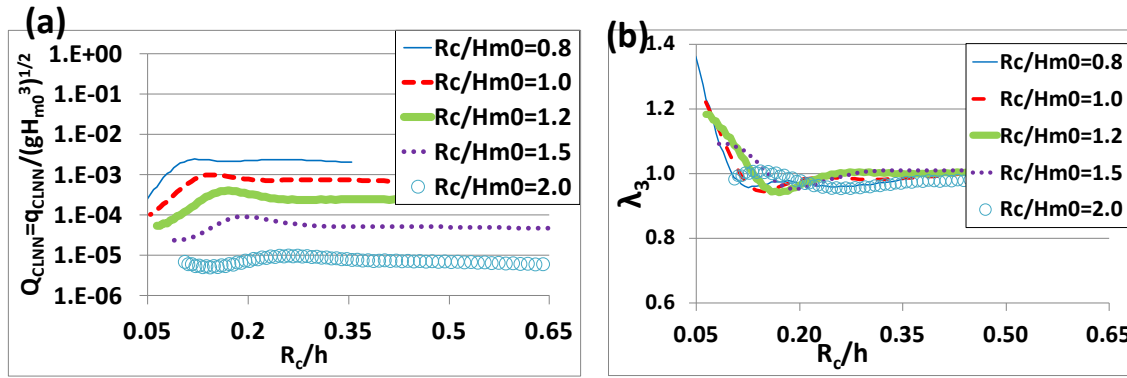
Fig. 8b.

Figure 8. Influence of R_c/h on overtopping: (a) CLASH NN model and (b) λ_3 term.

The overtopping prediction of *Q3* is given by:

$$\ln Q3 = \lambda_3 \ln Q2 = \left[a_3 + b_3 \cdot \exp\left(c_3 \cdot R_c / h \right) \right] \cdot \ln Q2 \tag{11}$$

where a_3 = 1.0; b_3 = 2.0 and c_3 = -35; rMSE$_{Q3}$ (CLdata) = 24.7% < 26.1% = rMSE$_{Q2}$ (CLdata) and

rMSE$_{Q3}$ (NNdata) = 20.4% < 21.8% = rMSE$_{Q2}$ (NNdata). Eq. (11) significantly improves the

overtopping prediction of Eq. (10) when 0.09 < R_c/h < 0.13; however, its effect is not significant

(Q3≈Q2) if R_c/h>0.13. Only 10 % of the CLdata fall in the range 0.09 < $X_3=R_c/h$ < 0.13. In the final

formula $X_3=R_c/h$ was considered because it significantly decreased rMSE$_{Q2}$ (CLdata) and rMSE$_{Q2}$

(NNdata). The predicted overtopping discharge increases if λ_3<1 (ln(Q1)<0).

Dimensionless armor crest berm width, $X_4 = G_c/H_{m0}$

Fig. 9a is a graphic representation of overtopping simulations using the CLASH NN. The higher

the $X_4=G_c/H_{m0}$, the greater the impact on overtopping. The explanatory term λ_4 is represented
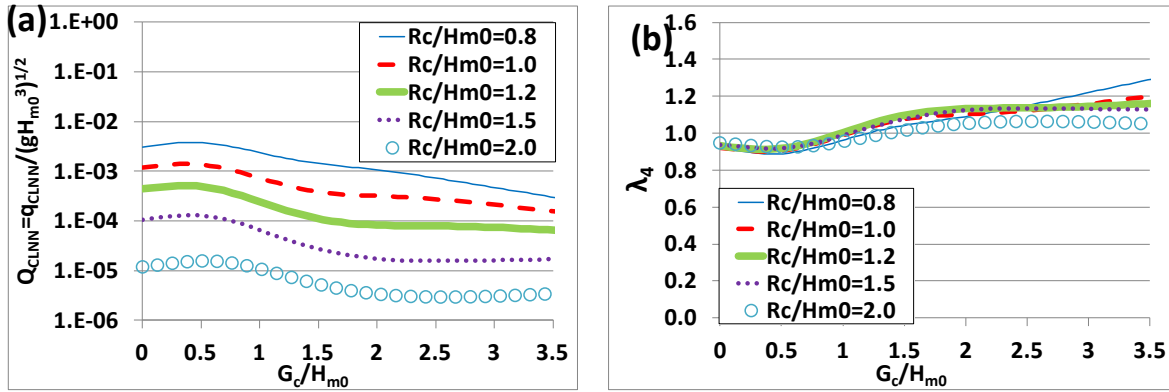
in Fig. 9b.

Figure 9. Influence of G_c/H_{m0} on overtopping: (a) CLASH NN model and (b) λ_4 term.

Eq. (12) gives the overtopping prediction of $Q4$, which considers the influence of the relative armor crest berm width:

$$\ln Q4 = \lambda_4 \ln Q3 = \max[c_4 ; (a_4 + b_4 \cdot G_c/H_{m0})] \cdot \ln Q3 \tag{12}$$

where $a_4 = 0.85$; $b_4 = 0.13$ and $c_4 = 0.95$; $rMSE_{Q4}$ (CLdata) = 21.4% < 24.7% = $rMSE_{Q3}$ (CLdata) and $rMSE_{Q4}$ (NNdata) = 16.2% < 20.4% = $rMSE_{Q3}$ (NNdata). Eq. (12) significantly improves the overtopping prediction of Eq. (11). $X_4 = G_c/H_{m0}$ is a relevant variable to explain the mean overtopping discharge on CMBW; when $G_c/H_{m0} > 0.75$, the higher the ratio G_c/H_{m0}, the lower the overtopping. The predicted overtopping discharge increases if $\lambda_4 < 1$ ($\ln(Q1) < 0$).

Dimensionless armor crest freeboard, $X_5 = A_c/R_c$

Fig. 10a is a graphic representation of overtopping simulations using the CLASH NN. The higher the $X_5 = A_c/R_c$, the greater the impact on overtopping. The explanatory term λ_5 is represented in Fig. 10b.
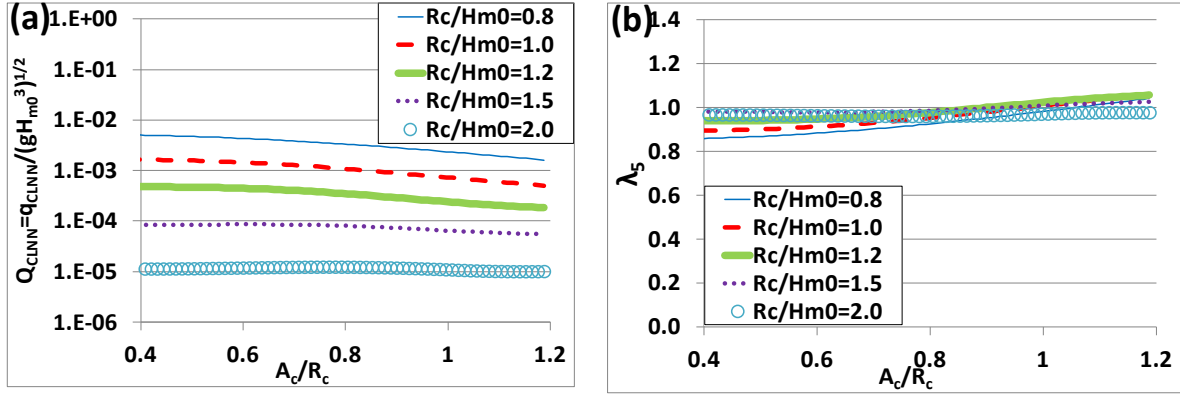
Figure 10. Influence of A_c/R_c on overtopping: (a) CLASH NN model and (b) λ_5 term.

Eq. (13) gives the overtopping prediction of $Q5$, that considers the influence of the relative armor crest freeboard:

$$\ln Q5 = \lambda_5 \ln Q4 = \left(a_5 + b_5 \cdot A_c/R_c\right) \cdot \ln Q4 \qquad (13)$$

where $a_5 = 0.85$ and $b_5 = 0.15$; $rMSE_{Q5}$ (CLdata) = 16.9% < 21.4% $rMSE_{Q4}$ (CLdata) and $rMSE_{Q5}$ (NNdata) = 10.6% < 16.2% = $rMSE_{Q4}$ (NNdata). Eq. (13) improves the overtopping prediction given by Eq. (12). $X_5 = A_c/R_c$ is a relevant variable to explain the mean overtopping discharge on CMBW; the higher the ratio A_c/R_c, the lower the overtopping. The predicted overtopping discharge increases if $\lambda_5 < 1$ ($\ln(Q1) < 0$).

Dimensionless toe berm: $X_6 = B_t/H_{m0}$ and $X_7 = h_t/H_{m0}$

The CMBW with concrete armor units usually has a toe berm with $X_7 = h_t/H_{m0}$ around 1.5 (see Grau, 2008). In the CLASH database, toe berms are controlled by B_t and h_t: if there is no toe berm, $B_t = 0$ and $h_t = h$. Two sets of simulations were conducted varying $X_6 = B_t/H_{m0}$ and $X_7 = h_t/H_{m0}$, respectively. The CLASH NN predictions were sensitive to the presence of a toe berm ($B_t > 0$). In the CLdata, 80% of the data represented CMBW without a toe berm ($B_t = 0$).

22

Fig. 11a is a graphic representation of overtopping simulations using the CLASH NN varying $X_7=h_t/H_{m0}$ with R_c/h=0.2. It is clear that the CLASH NN predictions detected the presence of a toe berm. Similar graphs were obtained for other values of R_c/h. The explanatory term λ_6 is represented in Fig. 11b.

Figure 11. Influence of h_t/H_{m0} on overtopping: (a) CLASH NN model and (b) λ_6 term.

If there is a toe berm (B_t >0), $X_3=R_c/h$ was a relevant variable to explain the overtopping prediction of the CLASH NN. The influence of the toe berm is described by:

$$\ln Q6 = \lambda_6 \ln Q5 = \begin{cases} \max[c_6;(a_6+b_6 \cdot R_c/h)] \cdot \ln Q5 & if \quad Bt > 0 \\ d_6 \cdot \ln Q5 & if \quad Bt = 0 \end{cases}. \tag{14}$$

where a_6 = 1.2; b_6 = -0.5 and $c_6=d_6=1$; $rMSE_{Q6}$ (CLdata) = 13.6% < 16.9% = $rMSE_{Q5}$ (CLdata) and $rMSE_{Q6}$ (NNdata) = 6.9% < 10.6% = $rMSE_{Q5}$ (NNdata). Eq. (14) improves the overtopping prediction of Eq. (13). Toe berm slightly reduces the overtopping discharge. The predicted overtopping discharge increases if λ_6<1 (ln($Q1$)<0).

Explicit overtopping formula for CMBW

Eqs. (8) to (14) can be used to define an explicit overtopping formula valid for CMBW in the ranges specified in Table 1. Eq. (15) integrates Eqs. (8) to (14). The predicted overtopping discharge increases if $\lambda_j < 1$ ($\ln(Q1) < 0$).

$$Q = \left(\frac{q}{\sqrt{g \cdot H_{m0}^3}} \right) = Q6 = \exp\left(\lambda_2 \cdot \lambda_3 . \lambda_4 \cdot \lambda_5 \cdot \lambda_6 \left[a_1 + b_1 \cdot \frac{R_c}{H_{m0}} \cdot \frac{1}{\gamma_f \gamma_\beta} \right] \right) \tag{15a}$$

where:

$$\lambda_2 = a_2 + b_2 \cdot \left(Ir \sqrt{R_c / H_{m0}} \right) \tag{15b}$$

$$\lambda_3 = a_3 + b_3 \cdot \exp(c_3 \cdot R_c / h) \tag{15c}$$

$$\lambda_4 = \max[c_4 ; a_4 + b_4 \cdot G_c / H_{m0}]; \tag{15d}$$

$$\lambda_5 = a_5 + b_5 \cdot A_c / R_c \tag{15e}$$

$$\lambda_6 = \begin{cases} \max[c_6 ; (a_6 + b_6 \cdot R_c / h)] & if \quad Bt > 0 \\ d_6 & if \quad Bt = 0 \end{cases} \tag{15f}$$

$$\gamma_\beta = \begin{cases} 1 - 0.0077|\beta| & for \ long-crested \ waves \\ 1 - 0.0058|\beta| & for \ short-crested \ waves \end{cases} \quad \text{valid for } \beta \leq 60° \tag{15g}$$

The influence of oblique wave attack was introduced using the obliquity factor γ_β given by Lykke-Andersen and Burcharth (2009) for rough slopes and validated in next section. Values for a_j, b_j, c_j and d_j are specified in Table 3.

Order (j)	a_j	b_j	c_j	d_j
1	-1.6	-2.6	0	0
2	1.20	-0.05	0	0
3	1.0	2.0	-35	0
4	0.85	0.13	0.95	0
5	0.85	0.15	0	0
6	1.2	-0.5	1	1

Table 3. Parameters a_j, b_j, c_j and d_j of Eq. (15).

According to Molines and Medina (2015), each formula must provide a list of roughness factors, since γ_f depends on the formula and the database used to calibrate the parameters for each one. Table 4 gives the roughness factors used in this paper. Using the γ_f given in Table 4, $rMSE_{Q6}$ (CLdata) = 12.1% and $rMSE_{Q6}$ (NNdata) = 5.1% are slightly different from the values 13.6% and 6.9% obtained using the best fitted γ_f for the CLASH NN model reported by Molines and Medina (2015).

Armor type	Overtopping estimator						
	Q_{VMJ}	$Q_{EurOtop}$	Q_{SZM}	Q_{JE}	Q_{VMB}	$Q6$	CLASH NN
Smooth	1.03	1.03	1.21	1.25	1.01	0.95	1.00
Rock (2L)	0.45	0.53	0.44	0.38	0.47	0.48	0.49
Cube (2L, random)	0.45	0.53	0.44	0.42	0.46	0.51	0.53
Cube (2L, flat)	0.48	0.53	0.51	0.46	0.48	0.52	0.53
Cube (1L, flat)	0.52	0.59	0.53	0.46	0.53	0.55	0.54
Antifer (2L)	0.50	0.57	0.51	0.44	0.50	0.52	0.52
Haro ^{R} (2L)	0.49	0.54	0.50	0.44	0.49	0.51	0.52
Tetrapod (2L)	0.43	0.52	0.39	0.37	0.43	0.45	0.42
Accropode ™ (1L)	0.48	0.51	0.49	0.42	0.49	0.48	0.48
Core-Loc™ (1L)	0.46	0.49	0.46	0.36	0.46	0.45	0.46
Xbloc ^{R} (1L)	0.47	0.49	0.48	0.42	0.47	0.46	0.51
Dolos (2L)	0.41	0.45	0.37	0.36	0.43	0.42	0.32
Cubipod$^®$ (2L)	0.55	0.57	0.45	0.36	0.57	0.47	0.45
Cubipod$^®$ (1L)	0.58	0.61	0.46	0.41	0.61	0.48	0.48

Note: (2L: 2 Layers), (1L: 1 Layer)

Table 4. Roughness factor (γ_f) used in this paper.

Eq. (15) has 16 parameters plus 14 roughness factors calibrated with 1,307 data (CLdata). In order to determine the uncertainty associated when using Eq. (15), it is convenient to calculate the final prediction error (FPE). The FPE takes into account not only MSE, but also the number of free parameters used in the formula and the number of data for calibration. According to Barron (1984), the final prediction error is FPE = MSE(1+2P/(N-P)); in this case, N=1,307 and P=(16+14)=30. The relative final prediction error (rFPE) is given by:

$$rFPE = \frac{FPE}{Var(\log Qo)} = rMSE\left(1 + \frac{2P}{N-P}\right) \tag{16}$$

where rMSE is the relative mean squared error given by Eq. (7); P is the number of calibrated parameters, and N is the number of data used for calibration. Therefore, one should expect

rMSE to be similar to rFPE = 12.1%*(1+2*30/(1,307-30)) = 12.7% when applying Eq. (15) to any

new data not included in CLdata, i.e. data not used to calibrate parameters.

In contrast, the CLASH NN is a "black-box" with 500 neural networks having 320 parameters

each and trained with 8,372 data (extracted from the CLASH database). The complexity of the

neural network structure makes it difficult to determine the rFPE. It is not possible to apply Eq.

(16) to the CLASH NN to estimate rFPE because bootstrapping was used to develop the neural

network model, and the neural network parameters may be correlated.

Confidence intervals for the overtopping formula

The confidence intervals for the overtopping formula Q6 given by Eq. (15) were calculated from

CLdata. Owen (1980) as well as Victor and Troch (2012) assumed that the logarithm of

dimensionless overtopping discharge follows a Gaussian distribution with constant variance. In

this paper, the variance was not considered as constant. To characterize the variance, it was

necessary to analyze the errors (ε^2=WF(ln$Q6$-ln$Q$[CLdata])^2) of the overtopping predictions from

Eq. (15), where WF is the weighting factor given in Table 2. Assuming a Gaussian error

distribution, the errors were ordered from the lowest to the highest value and grouped into

sets of consecutive 50 data. To characterize the variance of the errors, the

FPE=MSE*(1+2*30/(1,307-30)) for each 50 data group was calculated, resulting in higher FPE

when ln $Q6$ decreased. Thus, the error (ε) may be considered Gaussian-distributed with zero

mean and variance estimated by FPE:

$$FPE = \sigma^2(\varepsilon) = -0.15 \cdot \ln Q6 - 0.51 \qquad (17)$$

The 5% and 95% percentiles for the Q6 overtopping estimator, given by Eq. (15), may be

obtained by:

27

$$\ln Q\Big|_{5\%}^{95\%} = \ln Q6 \pm 1.65 \cdot \sqrt{-0.15 \cdot \ln Q6 - 0.51} \qquad\qquad (18)$$

Fig. 12a shows the 90% confidence interval for the overtopping estimator *Q6* compared to 1,307 CLdata (black circles, $\beta=0^0$) and 561 CLASH oblique wave data (red crosses, $10^0 \leq \beta \leq 60^0$). Fig. 12b compares the overtopping estimator Q6 to 1,307 NNdata (black circles, $\beta=0^0$) and 561 CLASH oblique wave data (red crosses, $10^0 \leq \beta \leq 60^0$).

The predictions of the overtopping estimator Q6 are accurate, especially in the range of high overtopping discharge, with a narrow 90% confidence interval. When applying Q6 with γ_f given in Table 4 and γ_β given by Eq. (15g), Figure 12.a shows good agreement for both perpendicular and oblique wave attack. One should note that oblique wave data were not used to build-up or calibrate Q6; however, Lykke-Andersen and Burcharth (2009) did use these data to calibrate γ_β given by Eq. (15g).
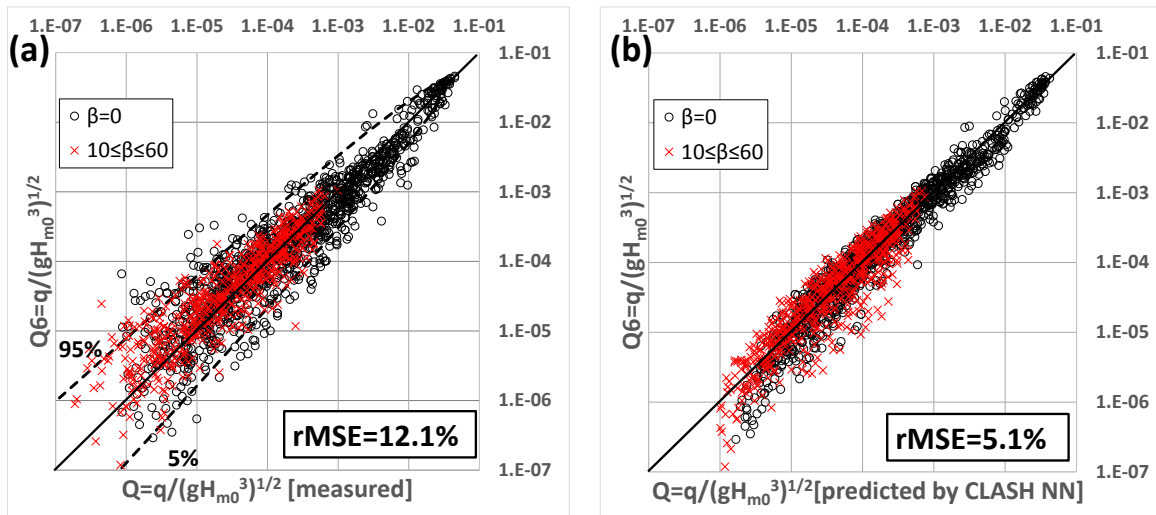

Figure 12. Q6 overtopping estimation and 90% confidence interval compared to (a) measured overtopping in CLASH, and (b) predicted overtopping by the CLASH NN.

Sensitivity analysis and applications of Q6

The influence of the explanatory terms λ_i (X_i), i=2 to 6, given in Eq. (15), on the original CLdata are analyzed here. Table 5 shows the maximum, minimum and coefficient of variation (CV) for each λ_i (X_i), i=2 to 6. The λ_2 (Ir) and λ_4 (G_c/H_{m0toe}) have a greater influence on the overtopping rate than λ_3 (R_c/h), λ_5 (A_c/R_c) and λ_6 (toe berm). The influence of λ_3 (R_c/h) is the lowest because its effect is only significant for deep armors (during construction phase).

λ_i (X_i), i=2 to 6	*Min*	*Max*	*CV(%)=$\sigma/\bar{\lambda_i}$*
λ_2 (Ir)	0.64	1.13	6.5
λ_3 (R_c/h)	1.00	1.10	1.6
λ_4 (G_c/H_{m0})	0.95	1.30	6.7
λ_5 (A_c/R_c)	0.86	1.06	3.2
λ_6 (toe berm)	1.00	1.14	3.2

Table 5. Ranges of the explanatory terms in CLdata used in Q6 given by Eq. (15)

Burcharth et al. (2014) presented examples of how coastal defense structures can be upgraded to withstand increased loads caused by climate change. Q6 can be used in the preliminary design stage to quantify the influence on overtopping when alternative geometrical modifications are made to existing CMBW. Analyzing a case similar to that described by EurOtop (2007), with parameters (see Fig. 2): β=0°; H_{m0}(m)=5; $T_{-1,0}$(s)=9; R_c(m)=5; A_c(m)=4; G_c(m)=5; $cot\alpha$=1.5; γ_f [cube, 2Layers, randomly-placed] =0.51 and h(m)=12 with toe berm (B_t (m)=4 and h_t(m)=9), the predicted overtopping discharge is $q(l/s/m)$=49. Four scenarios are considered in Fig. 13 to reduce overtopping discharge in the initial design: (1) higher structure

freeboard (both R_c and A_c); (2) higher crown wall freeboard (R_c); (3) higher armor crest freeboard (A_c) and (4) wider armor crest berm (G_c). Fig. 13 illustrates the effectiveness of each scenario, being the most effective an increase in the structure freeboard (R_c and A_c) followed by increasing only the crown wall freeboard (R_c).
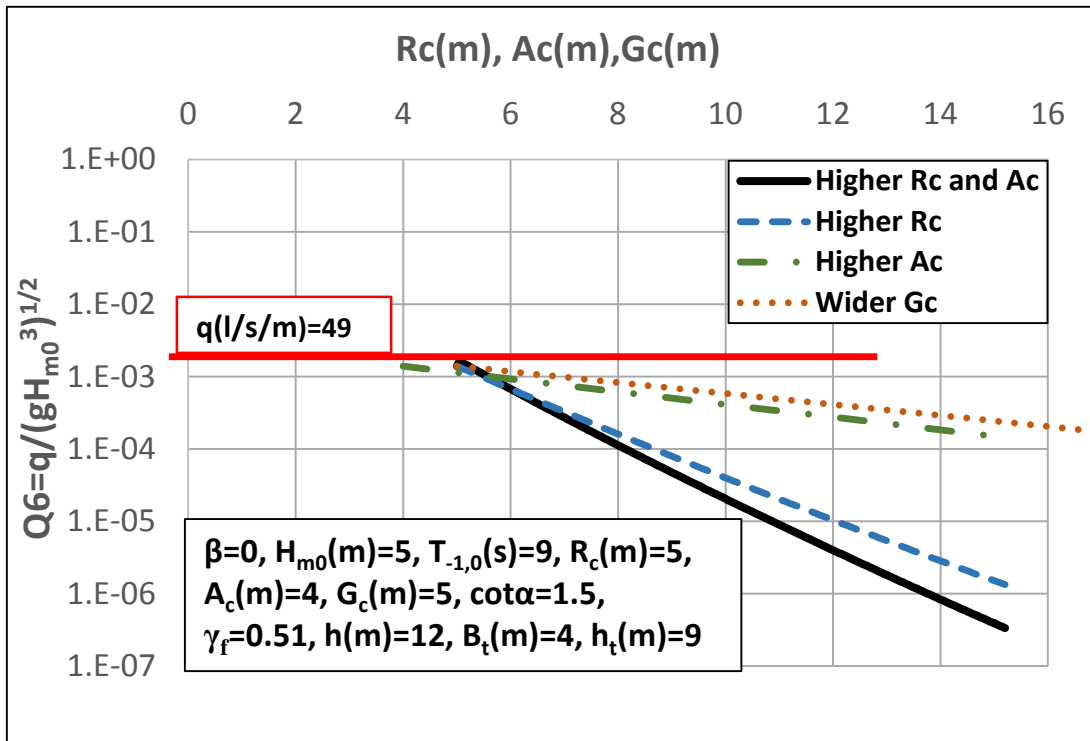

Figure 13. Sensitivity of CMBW geometrical changes to overtopping rate.

The effectiveness for each scenario given in the previous analysis does not take into account the cost of each geometrical change. A cost-effective change would require considering simultaneously the overtopping-reduction effectivity and the cost associated with each alternative, which would be dependent on the construction site and the logistical constraints.

Comparison to overtopping estimators given in the literature

Wave overtopping predictors were compared using the same CLdata and NNdata. Each estimator was used with the optimum roughness factor, γ_f, given in Table 4. Table 6 indicates the reference, overtopping model, number of parameters, explanatory variables, rMSE calculated using Eq. (7) on CLdata and NNdata and rFPE calculated using Eq.(16) on CLdata.

rMSE measures the goodness of fit of overtopping estimators to the target data. However, when comparing different overtopping estimators, it is better to use rFPE, which measures the expected error for new data not used during calibration. rFPE considers the rMSE, the number of parameters of each estimator and the number of data used for calibration.

Considering the results given in Table 6, *Q6* shows a behavior similar to the CLASH NN, but provides explicit relationships between explanatory variables and overtopping. Q6 has the lowest rFPE and hence it is the best estimator. Q_{VMB} provided the highest rFPE, but one should take into consideration that the CLASH tests selected for this study (CLdata ranges given in Table 1) fall in the range $0.52 < R_c/H_{m0} < 3.75$. Therefore, using Q_{VMB} does not take advantage of its better performance for zero and low crown wall freeboard cases ($0.00 < R_c/H_{m0} < 0.50$).

Reference	Overtopping model	Number of parameters	Explanatory variables	rMSE (CLdata)	rFPE (CLdata)	rMSE (NNdata)
Van der Meer and Janssen (1994)	Q_{VMJ}	2	γ_f, γ_β, X_1	27.4%	28.1%	22.9%
EurOtop (2007)	Cr^*Q_{VMJ}	5	γ_f, γ_β, X_1, X_4	23.7%	24.4%	17.9%
Smolka et al. (2009)	Q_{SZM}	4	γ_f, X_1, X_2, X_5	17.5%	18.0%	10.1%
Jafari and Etemad-Shahidi (2012)	Q_{JE}	11	γ_f, γ_β, X_1, X_2, X_4 $\tan\alpha$	23.7%	24.6%	16.2%
Van der Meer and Bruce (2014)	Q_{VMB}	3	γ_f, γ_β, X_1	34.9%	35.8%	33.4%
This paper	$Q6$	16	γ_f, γ_β, X_1 to X_7	12.1%	12.7%	5.1%
Van Gent et al. (2007)	CLASH NN	500 x 320	γ_f, R_c, A_c, G_c, $\cot\alpha_u$, $\cot\alpha_d$, B_t, B, h_B, $\cot\alpha_b$, h, h_t, H_{m0}, $T_{-1,0}$, β	8.1%	-	0%

Table 6. Comparison of overtopping estimators using CLdata and NNdata.

Conclusions

This paper describes a methodology to build-up a CLASH neural network-derived formula and confidence intervals to estimate mean overtopping discharge on conventional mound breakwaters. The new formula explicitly includes six explanatory dimensionless variables *(R_c/H_{m0}, Ir, R_c/h, G_c/H_{m0}, A_c/R_c and a toe berm variable based on R_c/h)* and two reduction factors (γ_f given in Table 4 and γ_β given by Lykke-Andersen and Burcharth, 2009).

The 16 parameters of the new overtopping estimator $Q6$ given by Eq. (15) were calibrated to minimize: (1) rMSE corresponding to overtopping measurements given in the CLASH database (CLdata), (2) rMSE corresponding to overtopping predictions given by the CLASH neural network (NNdata) and (3) the number of significant figures. The final result is a consistent and robust overtopping formula which reasonably emulates the CLASH neural network predictions for conventional mound breakwaters, with $rFPE_{Q6}$ (CLdata) = 12.7%. The 90% confidence interval for the overtopping estimations of $Q6$ is given by Eq.(18). The influence of short-crested and long-crested oblique waves on overtopping was introduced using Q6 with the correction factor (γ_β) developed within the CLASH EU-Project valid for rough slopes and $\beta \leq 60°$.

A sensitivity analysis was carried out to determine the effect of conventional mound breakwater geometrical changes on overtopping discharge. Four different scenarios were considered for an initial design: (1) higher structure freeboard (R_c and A_c); (2) higher crown wall freeboard (R_c); (3) higher armor crest freeboard (A_c) and (4) wider armor crest berm (G_c). A simultaneous increase in both R_c and A_c was most efficient to decrease overtopping discharge followed by increasing only the R_c. A cost analysis should be carried out for each specific conventional mound breakwater to determine the most cost-effective geometrical change to reduce overtopping, because geometrical changes in different variables may lead to considerable differences in cost, depending on the construction site and logistical constraints. $Q6$ describes explicit relationships between input variables and overtopping discharge and hence it facilitates use in engineering design to identify cost-effective solutions and to quantify the influence of variations in wave and structural parameters.

Compared to other overtopping models, *Q6* provides excellent results using CLdata and NNdata. The predictions of *Q6* are reasonably accurate for conventional mound breakwaters in the design phase. The new overtopping formula *Q6*, valid for conventional mound breakwaters in non-breaking conditions, gives overtopping predictions similar to those provided by the CLASH neural network; $rMSE_{Q6}$ [NNdata] = 5.1%. The CLASH neural network does provide slightly better estimations; however, it is a "black-box". By contrast, the new formula explicitly describes the influence of the γ_f, γ_β and the six dimensionless variables on dimensionless overtopping (*Q)*. Overtopping discharge on conventional mound breakwaters is greater if (1) R_c/H_{m0} decreases; (2) *Ir* increases; (3) R_c/h increases; (4) G_c/H_{m0} decreases, or (5) A_c/R_c decreases. The overtopping discharge is somewhat lower when placing a toe berm (B_t>0). Additionally, the higher the γ_f or γ_β, the greater the overtopping discharge.

Acknowledgments

References

Aminti, P. and Franco, L. (1988). "Wave overtopping on rubble mound breakwaters." *Proceedings 21st International Conference on Coastal Engineering,* ASCE, Vol. 1, 770-781.

Barron, A. (1984). "Predicted squared error. A criterion for automatic model selection." In S. Farlow (ed.), *Self-Organizing Methods in Modelling*, Marcel Dekker, 87-103.

Besley, P. (1999). "Overtopping of sea-walls-design and assessment manual." *R & D Technical Report 178*, Environment Agency, Bristol, UK.

Bradbury, A.P. and Allsop N.W.H. (1988). "Hydraulic effects of breakwater crown walls." *Design of Breakwaters*, ICE, Thomas Telford, 385-396.

Bruce, T., Van der Meer, J.W., Franco, L. and Pearson, J.M. (2006). "A comparison of overtopping performance of different rubble mound breakwater armours." *Proceedings 30th International Conference on Coastal Engineering*, World Scientific, Vol. 5, 4567-4579.

Bruce, T., Van der Meer, J.W., Franco, L. and Pearson, J.M. (2009). "Overtopping performance of different armour units for rubble mound breakwaters." *Coastal Engineering*, 56 (2), 166-179.

Burcharth, H.F., Lykke-Andersen, T. and Lara, J. L. (2014). "Upgrade of coastal defense structures against increased loadings caused by climate change: A first methodological approach." *Coastal Engineering*, 87, 112-121.

Coeveld, E.M., Van Gent, M.R.A. and Pozueta, B. (2005). *Neural Network, Manual NN_OVERTOPPING 2.0*. CLASH: Workpackage 8, http://www.clash.ugent.be/ (Accessed: December 2014).

Etemad-Shahidi, A., and Jafari, E. (2014). "New formulae for prediction of wave overtopping at inclined structures with smooth impermeable surface." *Ocean Engineering,* 84, 124-132.

EurOtop (2007). *Wave Overtopping of Sea Defences and Related Structures: Assessment Manual (EurOtop Manual)*. Pullen, T., Allsop, N.W.H., Bruce, T., Kortenhaus, A., Schüttrumpf, H. and Van der Meer, J.W. Environment Agency, UK/ENW Expertise Netwerk Waterkeren, NL/KFKI

Kuratorium für Forschung im Küsteningenieurwesen, Germany, http://www.overtopping-manual.com (Accessed: December 2014).

Garrido, J. M. and Medina, J.R. (2012). "New neural-network derived empirical formulas for estimating wave reflection on Jarlan-type breakwaters." *Coastal Engineering,* 62 (1), 9-18.

Grau, J.I. (2008). "Experiencias en obras portuarias. Recomendaciones para el diseño y la ejecución." *III Congreso Nacional de la Asociación Técnica de Puertos y Costas*, Puertos del Estado, 13-60 (in Spanish).

Hebsgaard, M., Sloth, P., and Juul, J. (1998). "Wave overtopping of rubble mound breakwaters." *Proceedings 26th International Conference on Coastal Engineering*, ASCE, Vol. 3, 2235-2248.

Jafari, E. and Etemad-Shahidi, A. (2012). "Derivation of a new model for prediction of wave overtopping at rubble mound structures." *Journal of Waterway, Port, Coastal, and Ocean Engineering*, 138 (1), 42-52.

Lykke-Andersen, T. and Burcharth, H.F. (2004). *D24 Report on additional tests Part A: Effect of obliqueness, short-crested waves and directional spreading.* CLASH: Workpackage 4, http://www.clash.ugent.be/ (Accessed: December 2014).

Lykke-Andersen, T. and Burcharth, H.F. (2009). "Three-dimensional investigations of wave overtopping on rubble mound structures". *Coastal Engineering*, 56, 180-189.

Medina, J.R., González-Escrivá, J.A., Garrido, J.M. and de Rouck, J. (2002). "Overtopping analysis using neural networks." *Proceedings 28th International Conference on Coastal Engineering*, World Scientific, Vol. 2, 2165-2177.

Molines, J. and Medina, J.R. (2015). "Calibration of overtopping roughness factors for concrete armor units in non-breaking conditions using the CLASH database." *Coastal Engineering,* 96, 62-70.

Molines, J., Pérez, T.J., Zarranz, G. and Medina, J.R. (2012). "Influence of cube and Cubipod® armor porosities on overtopping." *Proceedings 33rd International Conference on Coastal Engineering*, Coastal Engineering Research Council (ASCE), Paper No. 43/structures (Online), http://dx.doi.org/10.9753/icce.v33.structures.43.

Owen, M.W. (1980). "Design of sea walls allowing for wave overtopping." *Rep. EX 924*, Hydraulics Research, Wallingford, U.K.

Pedersen, J. (1996). "Wave forces and overtopping on crown walls of rubble mound breakwaters." Series paper 12, Hydraulic and Coastal Engineering Laboratory, Department of Civil Engineering, Aalborg University, Denmark.

Smolka, E., Zarranz, G. and Medina, J.R. (2009). "Estudio Experimental del Rebase de un Dique en Talud de Cubípodos." *X Jornadas Españolas de Costas y Puertos*, Universidad de Cantabria-Adif Congresos, 803-809 (in Spanish).

Stewart, T.P., Newberry, S.D., Simm, J.D. and Latham, J.P. (2002). "The hydraulic performance of tightly packed rock armour layers." *Proceedings 28th International Conference on Coastal Engineering*, World Scientific, Vol. 2, 1449–1471.

U.S. Army Corps of Engineers. USACE (2002). *Coastal Engineering Manual. Engineer Manual 1110-2-1100*. U.S. Army Corps of Engineers, Washington, D.C. (in 6 volumes).

Van der Meer, J.W. and Bruce, T. (2014). "New Physical Insights and Design Formulas on Wave Overtopping at Sloping and Vertical Structures." *Journal of Waterway, Port, Coastal and Ocean Engineering,* 140 (6), 04014025.

Van der Meer, J.W. and Janssen, J.P.F.M. (1994). "Wave Run-Up and Wave Overtopping at Dikes." Delft Hydraulics No. 485.

Van der Meer, J.W., Verhaeghe, H. and Steendam, G.J. (2009). "The new wave overtopping database for coastal structures." *Coastal Engineering,* 56 (2), 108-120.

Van Doorslaer, K., De Rouck, J., Audenaert, S. and Duquet, V. (2015). "Crest modifications to reduce wave overtopping of non-breaking waves over a smooth dike slope." *Coastal Engineering*, http://dx.doi.org/10.1016/j.coastaleng.2015.02.004 (in press).

Van Gent, M.R.A., van den Boogaard, H.F.P., Pozueta, B. and Medina, J.R. (2007). "Neural network modelling of wave overtopping at coastal structures." *Coastal Engineering,* 54 (8), 586–593.

Verhaeghe, H., van der Meer, J.W., Steendam, G.J., Besley, P., Franco, L. and Van Gent, M.R.A. (2003). "Wave overtopping database as the starting point for a neural network prediction method." *Proceedings Coastal Structures 2003,* ASCE, 418–430.

Victor, L. and Troch, P. (2012). "Wave overtopping at smooth impermeable steep slopes with low crest freeboards.*" Journal of Waterway, Port, Coastal, and Ocean Engineering*, 138 (5), 372-385.